Free Radical Biology and Medicine 58 (2013) 73–80

Contents lists available at SciVerse ScienceDirect

Free Radical Biology and Medicine

journal homepage: www.elsevier.com/locate/freeradbiomed

Original Contribution

Comprehensive pharmacokinetic studies and oral bioavailability of two Mn porphyrin-based SOD mimics, MnTE-2-PyP^{5+} and MnTnHex-2-PyP^{5+}

Tin Weitner [a], Ivan Kos [a,1], Huaxin Sheng [b,c], Artak Tovmasyan [a], Julio S. Reboucas [a,2], Ping Fan [d], David S. Warner [b,c], Zeljko Vujaskovic [a,3], Ines Batinic-Haberle [a], Ivan Spasojevic [d,*]

[a] Department of Radiation Oncology, Duke University Medical Center, Durham, NC 27710, USA
[b] Department of Anesthesiology, Duke University Medical Center, Durham, NC 27710, USA
[c] Multidisciplinary Neuroprotection Laboratories, Duke University Medical Center, Durham, NC 27710, USA
[d] Department of Medicine, Duke University Medical Center, Durham, NC 27710, USA

ARTICLE INFO

Article history:
Received 26 August 2012
Received in revised form
20 December 2012
Accepted 3 January 2013
Available online 15 January 2013

Keywords:
Pharmacokinetics
Oral availability
Mn porphyrins
MnTE-2-PyP^{5+}
MnTnHex-2-PyP^{5+}
SOD mimic
LC–MS/MS
Mouse plasma
Mouse organs
Free radicals

ABSTRACT

The cationic, *ortho* Mn(III) *N*-alkylpyridylporphyrins (alkyl=ethyl, E, and *n*-hexyl, *n*Hex) MnTE-2-PyP^{5+} (AEOL10113, FBC-007) and MnTnHex-2-PyP^{5+} have proven efficacious in numerous in vivo animal models of diseases having oxidative stress in common. The remarkable therapeutic efficacy observed is due to their: (1) ability to catalytically remove $O_2^{\bullet-}$ and $ONOO^-$ and other reactive species; (2) ability to modulate redox-based signaling pathways; (3) accumulation within critical cellular compartments, i.e., mitochondria; and (4) ability to cross the blood–brain barrier. The similar redox activities of both compounds are related to the similar electronic and electrostatic environments around the metal active sites, whereas their different bioavailabilities are presumably influenced by the differences in lipophilicity, bulkiness, and shape. Both porphyrins are water soluble, but MnTnHex-2-PyP^{5+} is approximately 4 orders of magnitude more lipophilic than MnTE-2-PyP^{5+}, which should positively affect its ability to pass through biological membranes, making it more efficacious in vivo at lower doses. To gain insight into the in vivo tissue distribution of Mn porphyrins and its impact upon their therapeutic efficacy and mechanistic aspects of action, as well as to provide data that would ensure proper dosing regimens, we conducted comprehensive pharmacokinetic (PK) studies for 24 h after single-dose drug administration. The porphyrins were administered intravenously (iv), intraperitoneally (ip), and via oral gavage at the following doses: 10 mg/kg MnTE-2-PyP^{5+} and 0.5 or 2 mg/kg MnTnHex-2-PyP^{5+}. Drug levels in plasma and various organs (liver, kidney, spleen, heart, lung, brain) were determined and PK parameters calculated (C_{max}, $C_{24\ h}$, $t_{max,}$ and AUC). Regardless of high water solubility and pentacationic charge of these Mn porphyrins, they are orally available. The oral availability (based on plasma AUC_{oral}/AUC_{iv}) is 23% for MnTE-2-PyP^{5+} and 21% for MnTnHex-2-PyP^{5+}. Despite the fivefold lower dose administered, the AUC values for liver, heart, and spleen are higher for MnTnHex-2-PyP^{5+} than for MnTE-2-PyP^{5+} (and comparable for other organs), clearly demonstrating the better tissue penetration and tissue retention of the more lipophilic MnTnHex-2-PyP^{5+}.

Introduction

MnTE-2-PyP^{5+} (AEOL10113, FBC-007), MnTnHex-2-PyP^{5+}, and MnTDE-2-ImP^{5+} (AEOL10150) have been the most frequently studied cationic metalloporphyrins in animal models of diseases that have oxidative stress in common [1–5]. The structures, aqueous physicochemical properties, and lipophilicity of MnTE-2-PyP^{5+} and MnTnHex-2-PyP^{5+} are summarized in Table 1,

Abbreviations: SOD, superoxide dismutase; MnP, Mn metalloporphyrin; MnTM-2-PyP^{5+}, Mn(III) *meso*-tetrakis(*N*-methylpyridinium-2-yl)porphyrin; MnTE-2-PyP^{5+}, Mn(III) *meso*-tetrakis(*N*-ethylpyridinium-2-yl)porphyrin, AEOL10113, FBC-007; MnTnHex-2-PyP^{5+}, Mn(III) *meso*-tetrakis(*N*-*n*-hexylpyridinium-2-yl)porphyrin; MnTnHep-2-PyP^{5+}, Mn(III) *meso*-tetrakis(*N*-*n*-heptylpyridinium-2-yl)porphyrin; MnTBAP^{3-}, Mn(III) *meso*-tetrakis(4-benzoic acid)porphyrin; MnTDE-2-ImP^{5+}, AEOL10150 Mn(III) *meso*-tetrakis(*N,N′*-diethylimidazolium-2-yl)porphyrin; LC–MS/MS, liquid chromatography–tandem mass spectrometry; MeCN, acetonitrile, PK, pharmacokinetics; ip, intraperitoneal; iv, intravenous; sc, subcutaneous; NF-kB, nuclear factor kB; $O_2^{\bullet-}$, superoxide; $ONOO^-$, peroxynitrite; $CO_3^{\bullet-}$, carbonate anion radical; ClO^-, hypochlorite; BBB, blood–brain barrier; AUC, area under the curve up to the last measurement at 24 h

* Corresponding author.
E-mail address: ivan.spasojevic@duke.edu (I. Spasojevic).
[1] Current address: Faculty of Pharmacy and Biochemistry, University of Zagreb, A. Kovacica 1, 10 000 Zagreb, Croatia.
[2] Current address: Departamento de Química, CCEN, Universidade Federal da Paraíba, João Pessoa, PB 58051-970, Brazil.
[3] Current address: Division of Translational Radiation Sciences, Department of Radiation Oncology, University of Maryland Baltimore, Baltimore, MD 21201.

0891-5849/$ - see front matter © 2013 Elsevier Inc. All rights reserved.
http://dx.doi.org/10.1016/j.freeradbiomed.2013.01.006

Table 1
Comparison of MnTE-2-PyP^{5+} and MnTnHex-2-PyP^{5+} with regard to their redox properties, reactivity toward superoxide and peroxynitrite, and lipophilicity.

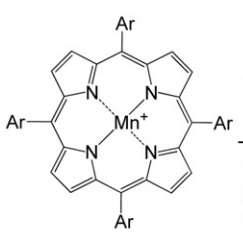

Ar	Ethyl	*n*-Hexyl
$E_{1/2}$ (mV vs NHE)	+228	+314
log k_{cat} ($O_2^{\bullet-}$)	7.76	7.48
log k_{red} ($ONOO^-$)	7.53	7.11
log k_{cat} ($CO_3^{\bullet-}$)	9.38	9.38
log P_{OW}	−7.79	−3.84

Redox property is expressed as the metal-centered reduction potential, $E_{1/2}$, for the $Mn^{III}P/Mn^{II}P$ redox couple, reactivity toward superoxide as log $k_{cat}(O_2^{\bullet-})$ and peroxynitrite as log $k_{red}(ONOO^-)$, and lipophilicity in terms of distribution between *n*-octanol and water, log P_{OW}. Data were taken from [1–3,7–9].

whereas their biologic and therapeutic effects are detailed elsewhere [1–4]. They were developed based on the structure–activity relationship between the metal-centered reduction potential, $E_{1/2}$, for the $Mn^{III}P/Mn^{II}P$ redox couple and the rate constant, k_{cat}, for the catalysis of $O_2^{\bullet-}$ dismutation [1–3,6]. The $k_{cat}(O_2^{\bullet-})$ parallels the rate constant for $ONOO^-$ reduction, k_{red} [1–3,7–9]. Such relationship is due to the similar thermodynamic and kinetic factors governing the reaction of electron-deficient cationic MnPs with electron-donating anionic species, such as $O_2^{\bullet-}$ and $ONOO^-$ [1–3,10]. The same is valid for their reactivity toward $CO_3^{\bullet-}$, ClO^-, and deprotonated, anionic cysteine sites of signaling proteins [2,3,9,11,12]. These MnPs are able to oxidatively modify the cysteine of p50 and p65 of NF-κB transcription factor, thereby preventing its activation [1,12,13].

The more lipophilic analogs with longer alkyl chains of up to 8 carbon atoms were synthesized with the goal of enhancing the bioavailability of MnPs while retaining the *ortho*-positioned pentacationic charge and in turn favorable redox properties [14,15]. MnTE-2-PyP^{5+} (2-carbon-atom ethyl chains) and MnTnHex-2-PyP^{5+} (6-carbon-atom *n*-hexyl chains) differ by ~4 orders of magnitude in lipophilicity (Table 1), which affects their mitochondrial distribution, transport across the BBB, and in turn their therapeutic effects [1,2,4,16–18]. Bioeffects differ less in magnitude (few to 120 folds) than the difference in lipophilicity would imply [16,19].

Pharmacokinetic studies provide invaluable information for researchers to understand the organ and cellular/subcellular accumulation and clearance of a drug and its mechanism of action. A limited rat PK study of MnTnHex-2-PyP^{5+} was performed recently [19], in a 90 min middle cerebral artery occlusion stroke model, in which rats were injected subcutaneously with 0.225 mg/kg twice daily for a week, starting at either 5 min or 6 h after reperfusion. The neurologic function was significantly improved and the total infarct size decreased with both early and delayed treatment. Naïve male Wistar rats were simultaneously given 75 μg/kg iv and 2.25 μg/kg sc of MnTnHex-2-PyP^{5+} every 24 h for 7 days. LC-MS/MS analysis of plasma and brain levels showed that the level of MnP in the brain steadily increases and at day 7 approaches the plasma level (25 nM in the brain vs 50 nM in plasma) [19]. This data set is the first to correlate directly the in vivo levels of MnP with its efficacy.

The common view is that hydrophilic drugs are not sufficiently orally available. The preliminary plasma PK set of data showed, surprisingly, that a highly hydrophilic MnTE-2-PyP^{5+} is orally available [20]. To increase our knowledge about the impact of charge and lipophilicity on Mn porphyrin bioavailability, we report herein a comprehensive pharmacokinetic study of two pentacationic metal complexes of very different lipophilicities (Table 1), MnTE-2-PyP^{5+} and MnTnHex-2-PyP^{5+}, administered via intravenous (iv), intraperitoneal (ip), and oral gavage (oral) routes.

Materials and methods

Porphyrins and other chemicals

MnTM-2-PyP^{5+} (λ_{max} 453.4 nm, log ε=5.11), MnTE-2-PyP^{5+} (λ_{max} 454.0 nm, log ε=5.14), MnTnHex-2-PyP^{5+} (λ_{max} 454.5 nm, log ε=5.21), and MnTnHep-2-PyP^{5+} (λ_{max} 454.0 nm, log ε=5.19) were synthesized and characterized as previously described [14,21]. Other chemicals used were acetonitrile (MeCN) from Fisher Scientific, methanol (anhydrous, absolute) from Mallinckrodt, glacial acetic acid from EM Science, heptafluorobutyric acid (HFBA) from Aldrich, and phosphate-buffered saline (50 mM sodium phosphate, 0.9% NaCl, pH 7.4) from Gibco.

Mice

The Duke University Medical Center Animal Facility has a program continuously accredited by AAALAC International. All experiments using animals were performed according to the approved protocol for humane care and use of animals. Ten-week-old C57BL/6 J female mice weighing 17–25 g were used. The concentration of aqueous solutions (for oral gavage) or saline solutions (for ip and iv injections) was adjusted so that the mice were injected with volumes of ~0.2 ml per dose. Mice did not have access to food 12 h or to water 3 h before oral gavage. In a dose-dependence study the mice were given orally 5 to 80 mg/kg MnTE-2-PyP^{5+} and 0.1 to 40 mg/kg MnTnHex-2-PyP^{5+} (see Supplementary Fig. S5). Mice were observed for 24 h and then euthanized and blood and organ samples were taken. In a time-dependence study, mice were given a single dose of 10 mg/kg MnTE-2-PyP^{5+} or 0.5 or 2 mg/kg MnTnHex-2-PyP^{5+}, via oral gavage or ip or iv, and were euthanized at various time points (5 min to 24 h). For the ip and iv studies 3 mice per time point sufficed. For the oral PK study there was a large variability at earlier time points. To increase accuracy, as many as 10 mice were used per time point up to 2 h after dosing, whereas for later time points 3 mice were sufficient. To collect tissues, mice were anesthetized with isoflurane, arterial blood was sampled, and the vasculature was briefly rinsed with 50 ml saline by transcardial perfusion before excision of liver, kidney, spleen, lung, heart, and brain. Plasma and hematocytes were separated immediately. Samples were kept at −80 °C.

Dosing of MnPs

In various efficacy studies performed thus far, MnPs have been administered as saline or phosphate-buffered saline solutions at various doses and via various routes: subcutaneous (sc), ip, iv, intramuscular, oral gavage, skin treatment, sc and iv osmotic pumps, and inhalation. At 3 mg/kg/day given ip for 4 days, MnTE-2-PyP^{5+} was able to fully reverse morphine tolerance in a mouse model [5]. In a rat lung pulmonary radioprotection study this drug nearly fully reversed lung fibrosis. It was given sc at 6 mg/kg/day for 2 weeks, starting at various time points after radiation, ranging from 2 h to 8 weeks [22,23]. MnTE-2-PyP^{5+} radiosensitized tumors when given ip at 6 mg/kg/day for 3 days [24]. At 15 mg/kg/day for 3 weeks (given in two daily increments), MnTE-2-PyP^{5+} exerted an anticancer effect in a 4T1 mouse mammary model [25]. In a rat diabetes model, 10 mg/kg given ip every second day from the onset of disease until completion of the study prevented adaptive transfer of autoimmune diabetes by a

diabetogenic T cell clone [26]. Therapeutic doses of MnTnHex-2-PyP^{5+} (established previously) for ranged from 0.05 to 3.2 mg/kg/day [1–3,27]. With twice daily sc injections at 1.6 mg/kg for up to 6 weeks, MnTnHex-2-PyP^{5+} exerted a remarkable brain tumor radio- and chemosensitizing effect in a D-245 MG sc xenograft Balb/c nu/nu mouse model [27,28]. At 0.05–0.3 mg/kg given sc daily for 2 weeks, starting at 2 h after radiation, this drug exerted pulmonary radioprotection in a rat model [22,23]. A 0.05 mg/kg single injection of MnTnHex-2-PyP^{5+} given iv 24 h before renal ischemia/reperfusion protected rat kidney [29]. When 0.12 mg/kg was given iv 30 min before and 30 min after 40 min uterus ischemia of a rabbit dam, a remarkable suppression of symptoms of cerebral palsy in pups was demonstrated [30].

In summary, the single doses of 10 mg/kg for MnTE-2-PyP^{5+} and 0.05 and 2 mg/kg for MnTnHex-2-PyP^{5+} were selected based on: (1) a dose-dependence study conducted herein; (2) doses frequently used after brief "pilot" acute toxicity tests for in vivo animal models of oxidative stress injuries, ranging from 3 to 15 mg/kg/day for MnTE-2-PyP^{5+} and 0.05 to 3.2 mg/kg/day for MnTnHex-2-PyP^{5+}; and (3) mouse heart mitochondria distribution studies in which mice were injected ip with 10 mg/kg MnTE-2-PyP^{5+} and 2 mg/kg MnTnHex-2-PyP^{5+} [22].

MnP plasma/tissue extraction

Organs were cryopulverized in a Bessman tissue pulverizer (BioSpec Products, Bartlesville, OK, USA) under liquid nitrogen and then homogenized in a rotary homogenizer (PTFE pestle and glass tube) with 2 vol of deionized water. An aliquot of either plasma or tissue homogenate was transferred into a 2-ml polypropylene screw-cap vial and a double volume of 1% acetic acid in methanol was added and mixed by vortexing for 30 s (1:2=homogenate:1% acetic acid in methanol). Samples were treated twice in the FastPrep apparatus (Qbiogene, Carlsbad, CA, USA) at speed 6.5 for 20 s and subsequently centrifuged 10 min at 13,000 *g* to separate proteins. An aliquot of the supernatant was pipetted into a 5-ml polypropylene tube (10 × 50 mm) and the solvent was completely removed in a Savant Speed-Vac evaporator at 40 °C within 1 h. The dry residue was dissolved in 20 μl of mobile phase B (see below) and sonicated for 5 min, then 80 μl of mobile phase B was added, and the mixture was sonicated again for 5 min and centrifuged for 5 min at 4500 *g* at 4 °C. Finally, the tube content was transferred to the HPLC autosampler polypropylene vial equipped with silicone/PTFE septum, followed by another cycle of centrifugation for 5 min at 4500 *g* (4 °C), after which the sample was immediately analyzed by LC–MS/MS.

LC–MS/MS

Quantitative analysis was performed on a Shimadzu 20 A series HPLC–Applied Biosystems MDS Sciex 3200 QTrap or 4000 QTrap tandem mass spectrometer at the pharmacology laboratory (Shared Resource PK/PD and Small Molecule Analysis Core) of Duke Cancer Center. The use of HFBA as an ion-pairing agent increases overall lipophilicity/volatility and greatly improves retention and ionization efficiency of the analytes, affording an abundance of $[MnP^{5+}+2HFBA^{-}]^{3+}$ and $[MnP^{5+}+3HFBA^{-}]^{2+}$ ions. Solvents employed were A, 95:5 H_2O:MeCN (0.1% HFBA), and B, MeCN (0.1% HFBA). MnTM-2-PyP^{5+} was used as an internal standard for determination of MnTE-2-PyP^{5+}, whereas MnTnHep-2-PyP^{5+} was used as an internal standard for determination of MnTnHex-2-PyP^{5+}. With the chosen solvent system all four atropoisomers of MnPs [31] collapsed into a single peak, enhancing the sensitivity of the method to as low as 0.5 ng/ml. Analyses were performed using a Phenomenex Luna C18 guard cartridge (i.d. × *L*, 2 × 4 mm) only. Specific mass transitions *m/z* $[MnP^{5+}+3HFBA^{-}]^{2+}$ to *m/z* $[MnP^{5+}-alkyl^{+}]$ fragmentation were followed: MnTE-2-PyP^{5+} (analyte) at *m/z* 713.3/363.6 and MnTM-2-PyP^{5+} (internal standard) at *m/z* 685.3/356.6; MnTnHex-2-PyP^{5+} (analyte) at *m/z* 825.5/611.5 and MnTnHep-2-PyP^{5+} (internal standard) at *m/z* 853.5/639.5. Calibration samples in the 1–300 nM or 0.1–30 μM range (depending on the expected levels of MnP) were prepared by adding known amounts of serially diluted pure standards into homogenates of the corresponding tissues and were analyzed along with study samples. Response was calculated as the ratio between the standard peak area and the internal standard peak area. The extraction of a lipophilic MnTnHex-2-PyP^{5+} and the preparation of the plasma and tissue samples for analysis were further improved in this study. Relative to MnTE-2-PyP^{5+}, the analysis of lipophilic MnPs is more difficult because of their affinity for proteins and plastic and glass surfaces. Thus, each MnP needed specific method adjustments as well as a different internal standard.

The excessive amounts of both drugs found in lung (the highest AUC values, Table 3) are probably due to imperfect perfusion (remaining blood visually observed). This is an inherent downside to our perfusion method in which the right atrium of the heart was cut for the blood outflow, thus lowering the perfusion pressure and causing insufficient lung perfusion. However, this perfusion method proved adequate for all other organs. On the other hand, the brain levels are low, approaching LLQ (lower limit of quantitation) values at 3.6 and 1.7 nM for MnTE-2-PyP^{5+} and MnTnHex-2-PyP^{5+}, respectively. Because of limitations of blood and tissue sample size and a need for high assay sensitivity, the PK studies were conducted with a discrete sampling scheme in which multiple mice were used for each time point.

Results and discussion

The comprehensive PK studies were conducted via iv, ip, and oral routes for MnTE-2-PyP^{5+} and MnTnHex-2-PyP^{5+} employing an LC–MS/MS method. The data for the levels of MnTE-2-PyP^{5+} in plasma and organs obtained with this high-throughput, less labor-consuming, and more sensitive method are in excellent agreement with the ip PK study on MnTE-2-PyP^{5+} reported previously that employed the HPLC/fluorescence assay developed in our laboratories [20].

Up to 10 mice per time point were used in the oral PK study to enhance the accuracy of analysis at earlier time points, at which the absorption of drug varied greatly among individual animals. Several strategies and tests were applied to decrease the large variability in the oral absorption among mice at earlier time points. They included: (1) a large number of animals at early time points (up to 10), (2) nonfasted vs fasted animals, and (3) mouth gavage by feeding needle vs gastric intubation with a polypropylene tubing inserted directly into the stomach. Regardless of the strategy employed, there was still a large variability observed between individual mice during the first couple of hours and it was reduced significantly at later time points. Therefore the maximal observed concentration (C_{max}), the time point at which C_{max} was achieved (t_{max}), and the half-life of MnP elimination obtained from the terminal slope of the PK curve (where available) ($t_{1/2\text{-elimination}}$) for oral administration suffer mostly from the accuracy point of view (because of large variability), whereas, on the other hand, the values of $C_{24\,h}$ (concentration at 24-h time point) are very low (except in the cases of liver and kidney). Thus, we found the AUC values (Table 2) to be the most reliable parameters to describe the difference in body exposure to the

two Mn porphyrins. Additional PK parameters are listed in the supplementary material (Figs. S1–S7, Table S1). Also shown herein are the plasma PK profiles (concentration vs time plots, Figs. 1 and 2), while the PK profiles of organs (liver, kidney, spleen, lung, heart, and brain) are given in the supplementary material (Figs. S1–S4).

PK profiles

The PK profiles (Figs. 1 and 2, Supplementary Figs. S1–S4) are presented as semilog plots to: (1) illustrate clearly the large data range—for instance, after oral gavage and over 24 h, the MnTE-2-PyP^{5+} levels in plasma ranged from 2 nM to almost 20 μM—and (2) demonstrate the complexity of the PK behavior—a simple single-exponential process should have appeared as a linear semilog plot and a nonlinear profile suggests a complex absorption/distribution/metabolism/elimination profile. Because of a limited number of time points, no attempt was made to fit a multicompartmental model to the data. Instead, the noncompartmental approach (WinNonlin; Pharsight, Inc.) was applied; the area under the 24-h PK curve was calculated by numerical integration and the $t_{1/2\text{-elimination}}$ calculated from the terminal slope of the PK curve (when accessible). Kinetic parameters for mice were calculated by modeling group mean data (i.e., the calculated average MnP levels at each time point). The standard deviations of the AUC values were estimated by the method of Bailer [32].

The PK profiles of MnTnHex-2-PyP^{5+} are characterized by higher t_{max} values, similar C_{max} values, and higher $C_{24\ h}$ relative to MnTE-2-PyP^{5+} (Supplementary Table S1), resulting in larger 24-h AUC values in most organs (Table 3).

Oral bioavailability

To ensure drug availability after oral administration, the integrity of compounds, in particular the metal site, must be preserved. Thus, no loss of metal center—where redox reactions of interest occur—should happen in the pH range from 1.5 (stomach) to 7.8. In very acidic, neutral, and moderately basic aqueous media, Mn(III) *N*-substituted pyridylporphyrins are remarkably stable—no metal is lost even in concentrated hydrochloric and sulfuric acids [14].

Bioavailability after oral administration (*f*, or *F* when expressed as %) is defined by Eq. (1) as a ratio, AUC_{oral}/AUC_{iv}, normalized by dose:

$$F = 100 \times [(AUC_{oral} \times dose_{iv})/(AUC_{iv} \times dose_{oral})] \quad (1)$$

This equation assumes linear pharmacokinetics (dose proportionality). The identical $dose_{iv}$ and $dose_{oral}$ of 10 mg/kg and related AUC values from Table 2 were used for calculation of oral availability of MnTE-2-PyP^{5+}. In the case of MnTnHex-2-PyP^{5+}, because of the toxicity-based limitation caused by blood pressure drop when injected intravenously, $dose_{iv}$ of 0.5 mg/kg and $dose_{oral}$ of 2 mg/kg were used to assess its oral availability, *F*. The data demonstrate an oral availability of 23% for MnTE-2-PyP^{5+} and 21% for MnTnHex-2-PyP^{5+}.

Organ distribution after oral and ip administration

Intravenous administration was used primarily to address the oral plasma bioavailability; yet the usefulness of this route is limited in experiments with small rodent. Intraperitoneal administration is more commonly used in efficacy studies as it closely resembles the iv route. Indeed, the plasma AUC_{ip} was 83% of AUC_{iv} for MnTE-2-PyP^{5+} and 84% for MnTnHex-2-PyP^{5+} (Table 2, Fig. 2). Thus, we performed comprehensive plasma and vital organ PK studies on both MnPs using ip and oral administration routes.

The oral availability of drugs to organs, calculated as AUC_{oral}/AUC_{ip} (Table 3, Fig. 3), ranges from 5 (kidney) to 46% (brain), for MnTE-2-PyP^{5+}, and 12 (heart) to 37% (liver), for MnTnHex-2-PyP^{5+}, confirming significant oral availability of both drugs. The important result here is that the delayed exposure of organs after

Table 2
The AUC values of MnTE-2-PyP^{5+} and MnTnHex-2-PyP^{5+} in plasma after intravenous, intraperitoneal, or oral administration.

MnP	Dose/ mg/kg	Plasma AUC (μM h)			Relative plasma AUC (%)		
		Iv	Ip	Oral	Ip vs iv	Oral vs ip	Oral vs iv
MnTE-2-PyP^{5+}	10	16.31 ± 0.1	13.46 ± 0.3	3.74 ± 0.6	83	28	23
MnTnHex-2-PyP^{5+}	2	—	5.69 ± 0.2	0.95 ± 0.1	—	17	—
MnTnHex-2-PyP^{5+}	0.5	1.12 ± 0.03	0.94 ± 0.01	0.085 ± 0.002	84	9	8

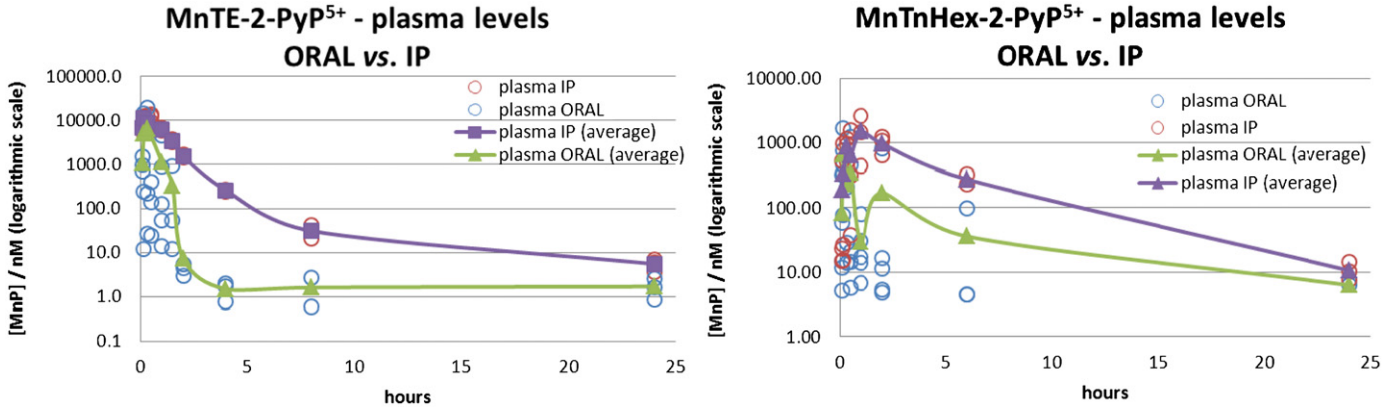

Fig. 1. Plasma pharmacokinetics of MnTE-2-PyP^{5+} (left) and MnTnHex-2-PyP^{5+} (right). Drug was given to female C57BL/6J mice at a single dose of 10 (MnTE-2-PyP^{5+}) or 2 mg/kg (MnTnHex-2-PyP^{5+}), either by oral or by ip route. Up to 10 mice were used for earlier time points in the oral PK study and 3 mice for all other time points; open circles are individual measurements. The PK curves for organs are given in the supplementary material.

Table 3
The AUC values of MnTE-2-PyP^{5+} and MnTnHex-2-PyP^{5+} for plasma, liver, kidney, heart, lung, brain, and spleen.

MnP	Sample	AUC ± σ (μM h)		AUC_{oral}/AUC_{ip} (%)
		Intraperitoneal	Oral	
MnTE-2-PyP^{5+} (10 mg/kg)	Plasma	13.46 ± 0.26	3.74 ± 0.62	28
	Liver	168.90 ± 4.82	39.25 ± 5.11	23
	Kidney	259.44 ± 8.32	12.25 ± 1.51	5
	Heart	4.30 ± 0.23	0.77 ± 0.07	18
	Lung[a]	10.09 ± 0.34	6.68 ± 0.72	66
	Brain	0.88 ± 0.01	0.40 ± 0.02	46
	Spleen	41.29 ± 2.44	6.78 ± 0.93	16
MnTnHex-2-PyP^{5+} (2 mg/kg)	Plasma	5.69 ± 0.21	0.95 ± 0.11	17
	Liver	178.64 ± 5.03	65.79 ± 16.70	37
	Kidney	58.98 ± 5.86	16.91 ± 5.97	29
	Heart	8.81 ± 0.30	1.04 ± 0.31	12
	Lung[a]	10.50 ± 0.29	58.31 ± 9.15	556
	Brain	0.52 ± 0.02	0.12 ± 0.01	24
	Spleen	49.46 ± 1.33	13.86 ± 3.71	28

The AUC values of MnTE-2-PyP^{5+} and MnTnHex-2-PyP^{5+} relate to the area under the curve up to the last measurement at 24 h (Fig. 1 and Supplementary Figs. S1–S4) and indicate the exposure of individual organs to the drug. The data are given in μM h. The μM relates to micromoles of MnP per 1000 ml of plasma or tissue homogenate. Using M_r of 965 or 1189 for MnTE-2-PyP^{5+} or MnTnHex-2-PyP^{5+} the values could be recalculated to be 1 μM = 0.97 μg/ml for the former or 1 μM = 1.19 μg/ml plasma or tissue homogenate for the latter MnP.

[a] The excessive amount found in the lungs is probably attributable to imperfect perfusion of this very vascular organ before its excision.

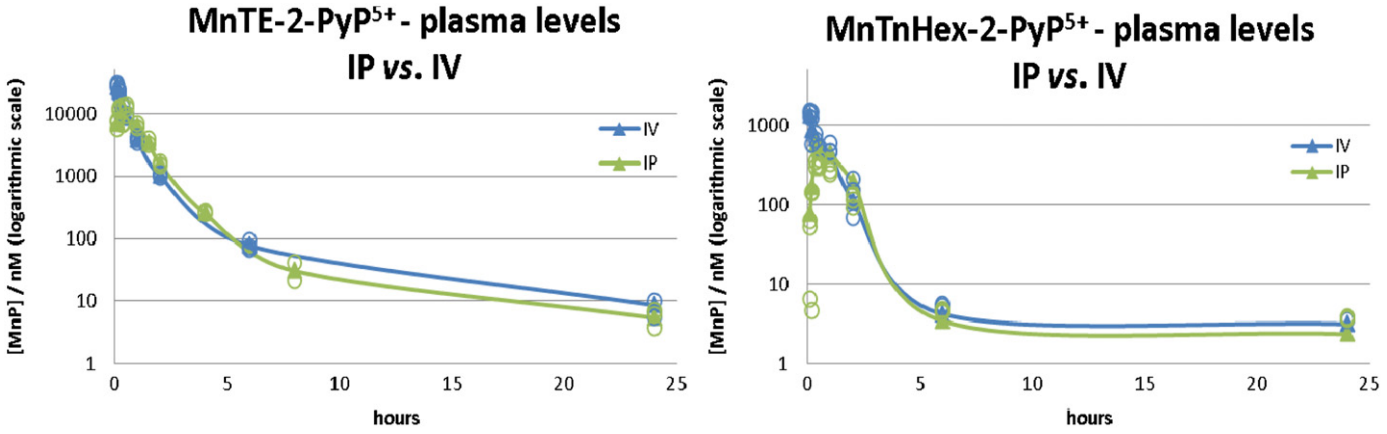

Fig. 2. Plasma pharmacokinetics via iv and ip routes for MnTE-2-PyP^{5+} (left) and MnTnHex-2-PyP^{5+} (right). For both compounds the AUC_{ip} is 83–84% of AUC_{iv}. Individual data points are given as open circles.

oral administration does not follow the same organ distribution pattern as after a rapid iv or ip plasma load. Pharmacokinetics (affinity and retention of the drug) of individual organs play an important role in how the drug will be distributed among individual organs after different administration routes. Furthermore, the calculated AUC values in Table 3 indicate that, at a fivefold lower dose, the exposure of organs to MnTnHex-2-PyP^{5+} is either higher than or comparable to MnTE-2-PyP^{5}. This clearly demonstrates the success in designing an analog with better tissue penetration and tissue retention.

At present, we cannot speculate much about the transport mechanism of these drugs. Both the lipophilicity and their charge will affect their distribution into the tissues and transport across the plasma membrane and BBB [33,34].

Dose dependence and acute toxicity

The dose-dependent distribution of MnPs in various organs after oral administration is provided in Supplementary Fig. S5. A linear dose dependence was observed for MnTE-2-PyP^{5+} levels in all organs. The liver and kidney are organs of high MnP accumulation, where saturation levels were achieved at doses above 40 mg/kg [20]. A similar trend was observed with MnTnHex-2-PyP^{5+}. At 10 mg/kg MnTE-2-PyP^{5+} either no or transient discomfort (subsiding within 15 min) was observed. At 20 and 40 mg/kg prolonged discomfort was observed, but mice recovered after 24 h. However, with 80 mg/kg the mice appeared very distressed and shivered immediately after drug delivery and were still distressed even 24 h after drug administration; the harvested organs (kidney, liver, and spleen) appeared abnormal. At ≥ 5 mg/kg of MnTnHex-2-PyP^{5+} mice appeared drowsy and were curled up and quiet for a while. Dose dependently, they recovered within 24 h after drug administration. At both 20 and 40 mg/kg MnTnHex-2-PyP^{5+} the mice exhibited strong shivering and one mouse died in each group. At 40 mg/kg all $C_{24\ h}$ values were lower than at 20 mg/kg. At such a high concentration the membranes that the MnP must cross to reach organs were probably compromised. The MnP thus entered the organs easily, but was as easily washed out when the mouse was perfused to extract blood-free organs. In another study, healthy mice were injected subcutaneously for a month at several doses of MnTnHex-2-PyP^{5+} in the range 0.2–5 mg/kg/day; the observed modest toxic effects include blood pressure

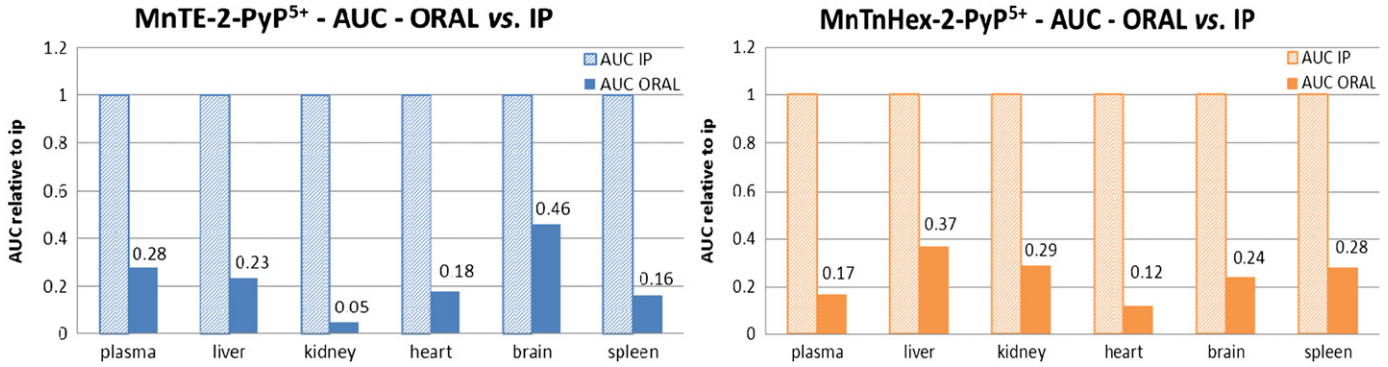

Fig. 3. The AUC_{oral} values relative to AUC_{ip} values for plasma, liver, kidney, heart, brain, and spleen of MnTE-2-PyP^{5+} and MnTnHex-2-PyP^{5+}. AUC_{ip} was taken as 100% (1 unit). Absolute values are given in Table 3.

drop, and brain, liver, kidney, and spleen toxicity which all disappeared within a drug-free month [4].

Pharmacokinetic studies of redox-active metal-based drugs of relevance to Mn(III) N-substituted pyridylporphyrins

Few studies have reported on the pharmacokinetics of synthetic redox-active drugs. Most often only plasma levels [35–37], and in very rare cases drug accumulation in organs or subcellular fragments have been reported [16,19,20,38–43]. Needless to say, the comprehensive PK studies are essential for understanding of the drug therapeutic effects. The failure of curcumin, a major curcuminoid of the popular Indian spice turmeric, in clinical trials on Alzheimer disease is the most obvious example. The drug was supposed to target brain, whereas it was not able to cross the BBB. Its poor bioavailability includes poor absorption, rapid metabolism, and rapid systemic elimination whereby it loses it redox potency. Such information should have been provided in preclinical studies [44,45].

PK plasma data are available for the MnSalen derivatives EUK-189 and EUK-207 when given via the sc route [37]. EUK-207 metal/ligand stability is increased via crown ether functionality [37], and its levels are higher in plasma than those of EUK-189. Thus, when given sc at 50 and 62.5 mg/kg, the reported C_{max} levels are ~4.6 and 1.4 μM for EUK-207 and EUK-189, respectively. Oral and ip PK studies and the in vitro efficacy of a lipophilic porphyrin, Mn(III) 5,10,15,20-tetrakis-ethylporphyrin (EUK-425) (log P_{OW}=0.93) were done, and PK profiles were provided, but not AUC values [35].

Limited data were reported in a cellular study of the distribution between cytosol and mitochondria of anionic $MnTBAP^{3-}$ and cationic MnTE-2-PyP^{5+} [46]. In a rat study, MnTDE-2-ImP^{5+} was injected intracerebroventricularly at 300 ng into a hemisphere. The brain parenchymal levels were reported in the collateral hemisphere [47]. Plasma PK of MnTDE-2-ImP^{5+} (AEOL10150) via HPLC/UV–Vis detection was reported when injected sc at 5 mg/kg [36].

MitoQ is a mitochondrially targeted redox-active compound and scavenger of a wide range of reactive species. It bears one positive charge and a 10-carbon atom hydrophobic chain and is vastly more lipophilic than either of the cationic MnPs studied herein (log P_{OW}=3.44 relative to log P_{OW}=−3.84 for MnTnHex-2-PyP^{5+} and −7.79 for MnTE-2-PyP^{5+}) [48]. Its oral availability is 10% [39]. The comparison of oral availability of very lipophilic MitoQ and very hydrophilic MnPs suggests that caution should be exercised when drawing conclusions on oral availability based upon drug hydrophilicity only.

Few other MnP-based scavengers of reactive species have been studied either for oral availability or oral efficacy, with limited PK data available, and are summarized here. Although they are not SOD mimics, they probably react with strong oxidants such as $ONOO^-$, ClO^-, $CO_3^{\bullet-}$ and $^{\bullet}NO_2$; limited data are available for such reactivities. Several highly lipophilic Mn(III) *meso*-tetracyclohexenylporphyrin analogs were orally active analgesics in a mouse model of carrageenan-induced thermal hyperalgesia. They were administered at 100 mg/kg either by ip route or orally; the actual drug levels and PK parameters have not been reported [49]. Although more lipophilic MnTnHex-2-PyP^{5+} might have been a better choice, the authors compared one of the studied lipophilic analogs with hydrophilic MnTE-2-PyP^{5+}, the latter being found ineffective orally at 100 mg/kg. Yet, in our hands, mice were seriously sick when MnTE-2-PyP^{5+} was given orally at 80 mg/kg (Supplementary Fig. S5), as discussed in the previous section, and such health conditions would preclude the evaluation of drug efficacy. A biscyclohexano-fused Mn(III) complex of bis(hydroxyphenyl)dipyrromethene, which contains one-half of a porphyrin molecule, was an orally active analgesic in a rat model of carrageenan-induced hyperalgesia [50]. At hour 2 after an injection of carrageenan, nearly 100% inhibition of thermal hyperalgesia was observed with 100 mg/kg oral dosing. The effect subsides at longer time points.

Conclusions

Although critical in drug discovery, the comprehensive pharmacokinetic data of redox-active drugs are scarce. Often only plasma and rarely a single organ accumulation are reported. Herein, in a detailed study, we provide the first evidence that the potent biocatalysts and redox regulators of cellular transcriptional activity, highly charged and fairly hydrophilic MnTE-2-PyP^{5+} and MnTnHex-2-PyP^{5+}, are orally available. The oral availability (AUC_{oral}/AUC_{iv}) is 23 and 21% for MnTE-2-PyP^{5+} and MnTnHex-2-PyP^{5+}, respectively. The AUC values for liver, kidney, heart, and spleen are higher for MnTnHex-2-PyP^{5+} than for MnTE-2-PyP^{5+} despite fivefold lower dose, clearly demonstrating the better tissue penetration and tissue retention of a more lipophilic MnTnHex-2-PyP^{5+}.

Acknowledgments

The authors acknowledge financial help from Duke University's CTSA Grant 1 UL 1 RR024128-01 from NCRR/NIH (A.T., I.B.H., I.S.); the W.H. Coulter Translational Partners Grant Program (I.B.H., I.S., A.T.); and NIH/NCI Duke Comprehensive Cancer Center Core Grant (5-P30-CA14236-29; I.S.), NIH U19AI067798 and I.B.H.

general research funds (A.T.). I.B.H., D.S.W., and I.S. are consultants with BioMimetix Pharmaceutical, Inc.

Appendix A. Supplementary material

Supplementary data associated with this article can be found in the online version at http://dx.doi.org/10.1016/j.freeradbiomed.2013.01.006.

References

[1] Batinic-Haberle, I.; Rajic, Z.; Tovmasyan, A.; Reboucas, J. S.; Ye, X.; Leong, K. W.; Dewhirst, M. W.; Vujaskovic, Z.; Benov, L.; Spasojevic, I. Diverse functions of cationic Mn(III) N-substituted pyridylporphyrins, recognized as SOD mimics. *Free Radic. Biol. Med.* **51:**1035–1053; 2011.

[2] Batinic-Haberle, I.; Reboucas, J. S.; Benov, L.; Spasojevic, I. Chemistry, biology and medical effects of water soluble metalloporphyrins. In: Kadish, K. M., Smith, K. M., Guillard, R., editors. *Handbook of Porphyrin Science*. Singapore: World Scientific; 2011. p. 291–393.

[3] Batinic-Haberle, I.; Reboucas, J. S.; Spasojevic, I. Superoxide dismutase mimics: chemistry, pharmacology, and therapeutic potential. *Antioxid. Redox Signaling* **13:**877–918; 2010.

[4] Tovmasyan, A.; Sheng, H.; Weitner, T.; Arulpragasam, A.; Lu, M.; Warner, D. S.; Spasojevic, I.; Batinic-Haberle, I. Design, mechanism of action, bioavailability and therapeutic effects of Mn porphyrin-based redox modulators. *Med. Princ. Pract.* (in press); 2012. http://dx.doi.org/10.1159/000341715.

[5] Batinic-Haberle, I.; Ndengele, M. M.; Cuzzocrea, S.; Reboucas, J. S.; Spasojevic, I.; Salvemini, D. Lipophilicity is a critical parameter that dominates the efficacy of metalloporphyrins in blocking the development of morphine antinociceptive tolerance through peroxynitrite-mediated pathways. *Free Radic. Biol. Med.* **46:**212–219; 2009.

[6] Batinic-Haberle, I.; Benov, L.; Spasojevic, I.; Fridovich, I. The ortho effect makes manganese(III) meso-tetrakis(N-methylpyridinium-2-yl)porphyrin a powerful and potentially useful superoxide dismutase mimic. *J. Biol. Chem* **273:**24521–24528; 1998.

[7] Ferrer-Sueta, G.; Batinic-Haberle, I.; Spasojevic, I.; Fridovich, I.; Radi, R. Catalytic scavenging of peroxynitrite by isomeric Mn(III) N-methylpyridylporphyrins in the presence of reductants. *Chem. Res. Toxicol.* **12:**442–449; 1999.

[8] Ferrer-Sueta, G.; Quijano, C.; Alvarez, B.; Radi, R. Reactions of manganese porphyrins and manganese-superoxide dismutase with peroxynitrite. *Methods Enzymol.* **349:**23–37; 2002.

[9] Ferrer-Sueta, G.; Vitturi, D.; Batinic-Haberle, I.; Fridovich, I.; Goldstein, S.; Czapski, G.; Radi, R. Reactions of manganese porphyrins with peroxynitrite and carbonate radical anion. *J. Biol. Chem.* **278:**27432–27438; 2003.

[10] Reboucas, J. S.; Spasojevic, I.; Tjahjono, D. H.; Richaud, A.; Mendez, F.; Benov, L.; Batinic-Haberle, I. Redox modulation of oxidative stress by Mn porphyrin-based therapeutics: the effect of charge distribution. *Dalton Trans.* **9:**1233–1242; 2008.

[11] Umile, T. P.; Groves, J. T. Catalytic generation of chlorine dioxide from chlorite using a water-soluble manganese porphyrin. *Angew. Chem. Int. Ed. Engl.* **50:**695–698; 2011.

[12] Batinic-Haberle, I.; Spasojevic, I.; Tse, H. M.; Tovmasyan, A.; Rajic St Z.; Clair, D. K.; Vujaskovic, Z.; Dewhirst, M. W.; Piganelli, J. D. Design of Mn porphyrins for treating oxidative stress injuries and their redox-based regulation of cellular transcriptional activities. *Amino Acids* **42:**95–113; 2012.

[13] Jaramillo, M. C.; Briehl, M. M.; Tome, M. E. Manganese porphyrin glutathionylates the p65 subunit of NF-κB to potentiate glucocorticoid-induced apoptosis in lymphoma. *Free Radic. Biol. Med.* **49:**S63; 2010.

[14] Batinić-Haberle, I.; Spasojević, I.; Stevens, R. D.; Hambright, P.; Fridovich, I. Manganese(III) *meso*-tetrakis(*ortho*-*N*-alkylpyridyl)porphyrins: synthesis, characterization, and catalysis of $O_2^{\bullet-}$ dismutation. *J. Chem. Soc. Dalton Trans.* :2689–2696; 2002.

[15] Rajic, Z.; Tovmasyan, A.; Spasojevic, I.; Sheng, H.; Lu, M.; Li, A. M.; Gralla, E. B.; Warner, D. S.; Benov, L.; Batinic-Haberle, I. A new SOD mimic, Mn(III) ortho *N*-butoxyethylpyridylporphyrin, combines superb potency and lipophilicity with low toxicity. *Free Radic. Biol. Med.* **52:**1828–1834; 2012.

[16] Miriyala, S.; Spasojevic, I.; Tovmasyan, A.; Salvemini, D.; Vujaskovic St Z.; Clair, D.; Batinic-Haberle, I. Manganese superoxide dismutase, MnSOD and its mimics. *Biochim. Biophys. Acta* **794-814:**2012; 1822.

[17] Spasojevic, I.; Li, A. M.; Tovmasyan, A.; Rajic, Z.; Salvemini St. D.; Clair, D.; Valentine, J. S.; Vujaskovic, Z.; Gralla, E. B.; Batinic-Haberle, I. Accumulation of porphyrin-based SOD mimics in mitochondria is proportional to their lipophilicity. *Free Radic. Biol. Med.* **49:**S199; 2010.

[18] Spasojevic, I.; Miryala, S.; Tovmasyan, A.; Salvemini, D.; Vujaskovic, Z.; Batinic-Haberle St. I.; Clair, D. Lipophilicity of Mn(III) *N*-alkylpyridylporphyrins dominates their accumulation within mitochondria and therefore in vivo efficacy: a mouse study. *Free Radic. Biol. Med.* **51:**S98; 2011.

[19] Sheng, H.; Spasojevic, I.; Tse, H. M.; Jung, J. Y.; Hong, J.; Zhang, Z.; Piganelli, J. D.; Batinic-Haberle, I.; Warner, D. S. Neuroprotective efficacy from a lipophilic redox-modulating Mn(III) N-hexylpyridylporphyrin, MnTnHex-2-PyP: rodent models of ischemic stroke and subarachnoid hemorrhage. *J. Pharmacol. Exp. Ther.* **338:**906–916; 2011.

[20] Spasojevic, I.; Chen, Y.; Noel, T. J.; Fan, P.; Zhang, L.; Reboucas St J. S.; Clair, D. K.; Batinic-Haberle, I. Pharmacokinetics of the potent redox-modulating manganese porphyrin, MnTE-2-PyP^{5+}, in plasma and major organs of B6C3F1 mice. *Free Radic. Biol. Med.* **45:**943–949; 2008.

[21] Kos, I.; Reboucas, J. S.; DeFreitas-Silva, G.; Salvemini, D.; Vujaskovic, Z.; Dewhirst, M. W.; Spasojevic, I.; Batinic-Haberle, I. Lipophilicity of potent porphyrin-based antioxidants: comparison of ortho and meta isomers of Mn(III) N-alkylpyridylporphyrins. *Free Radic. Biol. Med.* **47:**72–78; 2009.

[22] Gauter-Fleckenstein, B.; Fleckenstein, K.; Owzar, K.; Jiang, C.; Batinic-Haberle, I.; Vujaskovic, Z. Comparison of two Mn porphyrin-based mimics of superoxide dismutase in pulmonary radioprotection. *Free Radic. Biol. Med.* **44:**982–989; 2008.

[23] Gauter-Fleckenstein, B.; Fleckenstein, K.; Owzar, K.; Jiang, C.; Reboucas, J. S.; Batinic-Haberle, I.; Vujaskovic, Z. Early and late administration of MnTE-2-PyP5+ in mitigation and treatment of radiation-induced lung damage. *Free Radic. Biol. Med.* **48:**1034–1043; 2010.

[24] Moeller, B. J.; Batinic-Haberle, I.; Spasojevic, I.; Rabbani, Z. N.; Anscher, M. S.; Vujaskovic, Z.; Dewhirst, M. W. A manganese porphyrin superoxide dismutase mimetic enhances tumor radioresponsiveness. *Int. J. Radiat. Oncol. Biol. Phys.* **63:**545–552; 2005.

[25] Rabbani, Z. N.; Spasojevic, I.; Zhang, X.; Moeller, B. J.; Haberle, S.; Vasquez-Vivar, J.; Dewhirst, M. W.; Vujaskovic, Z.; Batinic-Haberle, I. Antiangiogenic action of redox-modulating Mn(III) meso-tetrakis(N-ethylpyridinium-2-yl)porphyrin, MnTE-2-PyP^{5+}, via suppression of oxidative stress in a mouse model of breast tumor. *Free Radic. Biol. Med.* **47:** 992–1004; 2009.

[26] Piganelli, J. D.; Flores, S. C.; Cruz, C.; Koepp, J.; Batinic-Haberle, I.; Crapo, J.; Day, B.; Kachadourian, R.; Young, R.; Bradley, B.; Haskins, K. A metalloporphyrin-based superoxide dismutase mimic inhibits adoptive transfer of autoimmune diabetes by a diabetogenic T-cell clone. *Diabetes* **51:** 347–355; 2002.

[27] Batinic-Haberle, I.; Keir, S. T.; Rajic, Z.; Tovmasyan, A.; Bigner, D. D. Lipophilic Mn porphyrins in the treatment of brain tumors. *Free Radic. Biol. Med.* **51:**S119; 2011.

[28] Batinic-Haberle, I.; Keir, S. T.; Rajic, Z.; Tovmasyan, A.; Spasojevic, I.; Dewhirst, M. W.; Bigner, D. D. Glioma growth suppression via modulation of cellular redox status by a lipophilic Mn porphyrin. Presented at the Mid-Winter SPORE Meeting. San Francisco, USA; 2011:31-32.

[29] Saba, H.; Batinic-Haberle, I.; Munusamy, S.; Mitchell, T.; Lichti, C.; Megyesi, J.; MacMillan-Crow, L. A. Manganese porphyrin reduces renal injury and mitochondrial damage during ischemia/reperfusion. *Free Radic. Biol. Med.* **42:**1571–1578; 2007.

[30] Drobyshevsky, A.; Luo, K.; Derrick, M.; Yu, L.; Du, H.; Prasad, P. V.; Vasquez-Vivar, J.; Batinic-Haberle, I.; Tan, S. Motor deficits are triggered by reperfusion–reoxygenation injury as diagnosed by MRI and by a mechanism involving oxidants. *J. Neurosci.* **32:**5500–5509; 2012.

[31] Spasojevic, I.; Menzeleev, R.; White, P. S.; Fridovich, I. Rotational isomers of N-alkylpyridylporphyrins and their metal complexes: HPLC separation, ^{1}H NMR and X-ray structural characterization, electrochemistry, and catalysis of $O_2^{\bullet-}$ disproportionation. *Inorg. Chem.* **41:**5874–5881; 2002.

[32] Bailer, A. J. Testing for the equality of area under the curves when using destructive measurement techniques. *J. Pharmacokinet. Biopharm* **16:**303–309; 1988.

[33] Murphy, M. P.; Smith, R. A. Targeting antioxidants to mitochondria by conjugation to lipophilic cations. *Annu. Rev. Pharmacol. Toxicol.* **47:**629–656; 2007.

[34] Saitoh, H.; Kawai, S.; Miyazaki, K.; Arita, T. Transport characteristics of propantheline across rat intestinal brush border membrane. *J. Pharm. Pharmacol.* **40:**176–180; 1988.

[35] Rosenthal, R. A.; Huffman, K. D.; Fisette, L. W.; Damphousse, C. A.; Callaway, W. B.; Malfroy, B.; Doctrow, S. R. Orally available Mn porphyrins with superoxide dismutase and catalase activities. *J. Biol. Inorg. Chem.* **14:**979–991; 2009.

[36] O'Neill, H. C.; White, C. W.; Veress, L. A.; Hendry-Hofer, T. B.; Loader, J. E.; Min, E.; Huang, J.; Rancourt, R. C.; Day, B. J. Treatment with the catalytic metalloporphyrin AEOL 10150 reduces inflammation and oxidative stress due to inhalation of the sulfur mustard analog 2-chloroethyl ethyl sulfide. *Free Radic. Biol. Med.* **48:**1188–1196; 2010.

[37] Rosenthal, R. A.; Fish, B.; Hill, R. P.; Huffman, K. D.; Lazarova, Z.; Mahmood, J.; Medhora, M.; Molthen, R.; Moulder, J. E.; Sonis, S. T.; Tofilon, P. J.; Doctrow, S. R. Salen Mn complexes mitigate radiation injury in normal tissues. *Anticancer Agents Med. Chem* **11:**359–372; 2011.

[38] Liang, L. P.; Huang, J.; Fulton, R.; Day, B. J.; Patel, M. An orally active catalytic metalloporphyrin protects against 1-methyl-4-phenyl-1,2,3,6-tetrahydropyridine neurotoxicity in vivo. *J. Neurosci.* **27:**4326–4333; 2007.

[39] Smith, R. A.; Murphy, M. P. Animal and human studies with the mitochondria-targeted antioxidant MitoQ. *Ann. N. Y. Acad. Sci.* **1201:**96–103; 2010.

[40] Spasojevic, I.; Chen, Y.; Noel, T. J.; Yu, Y.; Cole, M. P.; Zhang, L.; Zhao St Y.; Clair, D. K.; Batinic-Haberle, I. Mn porphyrin-based superoxide dismutase (SOD) mimic, MnIIITE-2-PyP5+, targets mouse heart mitochondria. *Free Radic. Biol. Med.* **42:**1193–1200; 2007.

[41] Smith, R. A.; Porteous, C. M.; Gane, A. M.; Murphy, M. P. Delivery of bioactive molecules to mitochondria in vivo. *Proc. Natl. Acad. Sci. USA* **100:**5407–5412; 2003.
[42] Sheng, H.; Enghild, J. J.; Bowler, R.; Patel, M.; Batinić-Haberle, I.; Calvi, C. L.; Day, B. J.; Pearlstein, R. D.; Crapo, J. D.; Warner, D. S. Effects of metalloporphyrin catalytic antioxidants in experimental brain ischemia. *Free Radic. Biol. Med.* **33:**947–961; 2002.
[43] Davis, R. M.; Mitchell, J. B.; Krishna, M. C. Nitroxides as cancer imaging agents. *Anti-Cancer Agents Med. Chem.* **11:**347–358; 2011.
[44] Anand, P.; Kunnumakkara, A. B.; Newman, R. A.; Aggarwal, B. B. Bioavailability of curcumin: problems and promises. *Mol. Pharm.* **4:**807–818; 2007.
[45] Baum, L.; Lam, C. W.; Cheung, S. K.; Kwok, T.; Lui, V.; Tsoh, J.; Lam, L.; Leung, V.; Hui, E.; Ng, C.; Woo, J.; Chiu, H. F.; Goggins, W. B.; Zee, B. C.; Cheng, K. F.; Fong, C. Y.; Wong, A.; Mok, H.; Chow, M. S.; Ho, P. C.; Ip, S. P.; Ho, C. S.; Yu, X. W.; Lai, C. Y.; Chan, M. H.; Szeto, S.; Chan, I. H.; Mok, V. Six-month randomized, placebo-controlled, double-blind, pilot clinical trial of curcumin in patients with Alzheimer disease. *J. Clin. Psychopharmacol.* **28:**110–113; 2008.
[46] Li, Q. Y.; Pedersen, C.; Day, B. J.; Patel, M. Dependence of excitotoxic neurodegeneration on mitochondrial aconitase inactivation. *J. Neurochem.* **78:**746–755; 2001.
[47] Sheng, H.; Enghild, J. J.; Bowler, R.; Patel, M.; Batinic-Haberle, I.; Calvi, C. L.; Day, B. J.; Pearlstein, R. D.; Crapo, J. D.; Warner, D. S. Effects of metalloporphyrin catalytic antioxidants in experimental brain ischemia. *Free Radic. Biol. Med.* **33:**947–961; 2002.
[48] James, A. M.; Cocheme, H. M.; Smith, R. A.; Murphy, M. P. Interactions of mitochondria-targeted and untargeted ubiquinones with the mitochondrial respiratory chain and reactive oxygen species: implications for the use of exogenous ubiquinones as therapies and experimental tools. *J. Biol. Chem* **280:**21295–21312; 2005.
[49] Rausaria, S.; Ghaffari, M. M.; Kamadulski, A.; Rodgers, K.; Bryant, L.; Chen, Z.; Doyle, T.; Shaw, M. J.; Salvemini, D.; Neumann, W. L. Retooling manganese(III) porphyrin-based peroxynitrite decomposition catalysts for selectivity and oral activity: a potential new strategy for treating chronic pain. *J. Med. Chem.* **54:**8658–8669; 2011.
[50] Rausaria, S.; Kamadulski, A.; Rath, N. P.; Bryant, L.; Chen, Z.; Salvemini, D.; Neumann, W. L. Manganese(III) complexes of bis(hydroxyphenyl)dipyrromethenes are potent orally active peroxynitrite scavengers. *J. Am. Chem. Soc.* **133:**4200–4203; 2011.